Communications

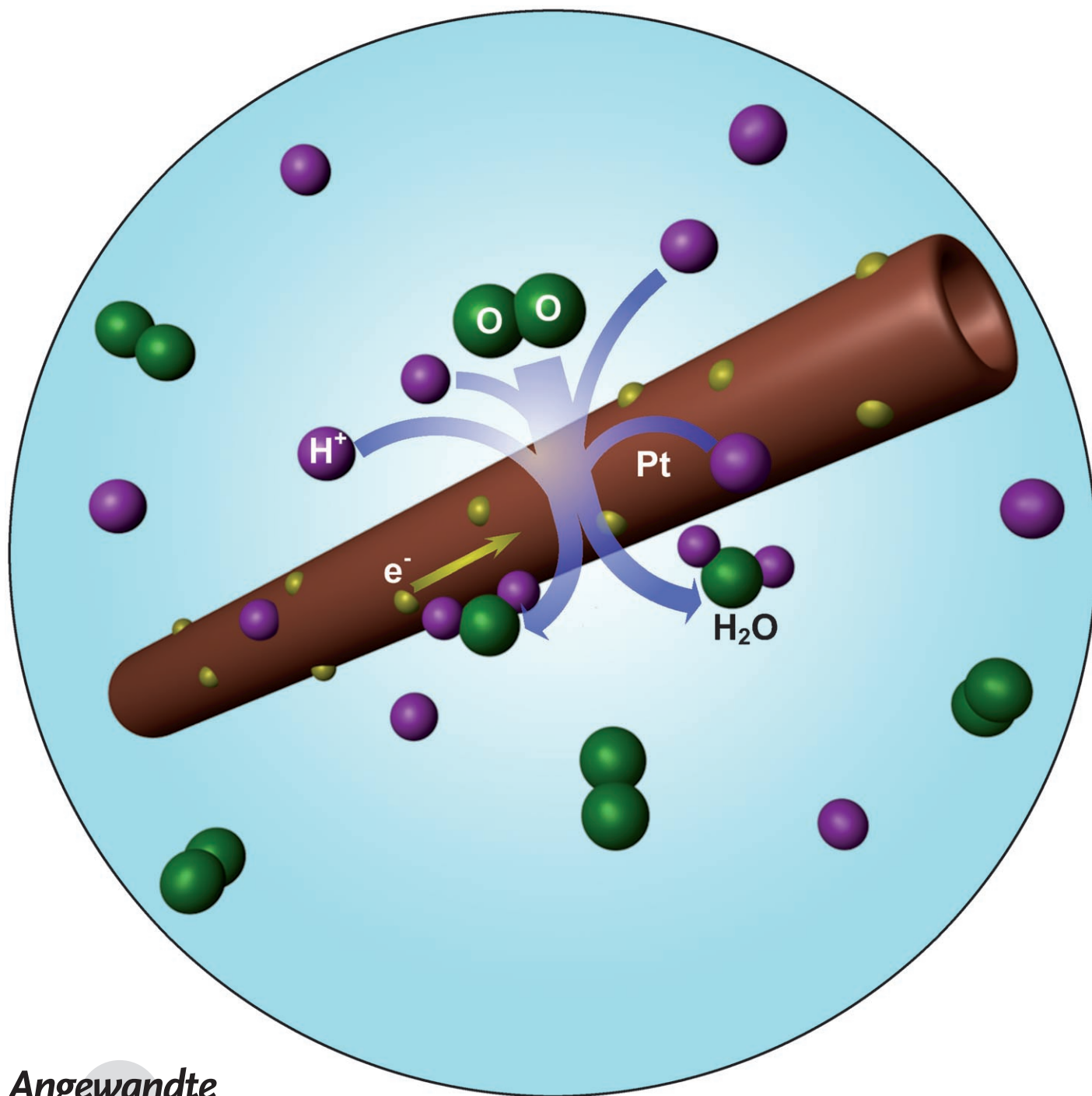# Supportless Pt and PtPd Nanotubes as Electrocatalysts for Oxygen-Reduction Reactions**

*Zhongwei Chen, Mahesh Waje, Wenzhen Li, and Yushan Yan**

Angewandte Chemie

Electrocatalyst durability has been recently recognized as one of the most important issues that must be addressed before the commercialization of proton exchange membrane fuel cells (PEMFCs).[1,2] The durability problem is particularly severe in the cathode, where the oxygen-reduction reaction (ORR) occurs. At present, the most widely used cathode catalyst system is platinum in the form of small nanoparticles (2–5 nm) supported on amorphous carbon-particle aggregates (Pt/C). The poor durability of the Pt/C catalyst is reflected by a fast and significant loss of platinum electrochemical surface area (ECSA) over time during fuel cell operation.[1,2] The mechanisms for the loss of platinum ECSA at the cathode have been discussed[1,2] and can be summarized as follows: 1) loss of platinum nanoparticles from the electrical contact because of corrosion of the carbon support, 2) platinum dissolution and redeposition or Ostwald ripening of the platinum nanoparticles, 3) platinum-nanoparticle aggregation driven by surface-energy minimization, and 4) platinum-nanoparticle dissolution and subsequent migration of the soluble Pt^{2+} species within the polymer electrolyte and the eventual chemical reduction by hydrogen crossed-over from the anode through the proton-exchange membrane.

The carbon-corrosion problem can be alleviated by the use of a more corrosion-resistant catalyst support, for example, graphitized-carbon materials or carbon nanotubes.[3] No effective solutions, however, exist for addressing the other three mechanisms. Our approach to a durable electrocatalyst is to develop supportless platinum nanotubes (PtNTs) and platinum-alloy nanotubes (e.g., platinum–palladium-alloy nanotubes (PtPdNTs)) as the cathode catalyst. Because of their unique combination of dimensions at multiple length scales, PtNTs and PtPdNTs can provide high platinum surface area by their nanometer-sized wall thickness (Figures S1 and S2 in the Supporting Information) without the need for a high-surface-area support (e.g., carbon black). At the same time, these materials have the potential to eliminate or significantly reduce all of the four degradation pathways discussed above as a result of their micrometer-sized length: First, PtNTs do not require a support, and thus the support-corrosion problem is eliminated. Second, the micrometer-sized length of the PtNTs (1D nanostructure) makes the PtNTs less vulnerable to dissolution, Ostwald ripening, and aggregation during fuel cell operation than the platinum

nanoparticles (0D nanostructure). Additionally, the PtNTs and PtPdNTs, like carbon nanotubes, have an anisotropic morphology that can improve mass transport and catalyst utilization.[3] And if properly assembled (e.g., cubic or hexagonal close-packing and vertical alignment on the nafion membrane), they can also lead to a thin catalyst layer (e.g., 0.5 μm at a PtNT wall thickness of 2 nm and a platinum loading of 0.2 mg cm^{-2}; Figure S3), further improving the mass-transfer characteristics within the catalyst layer.[4]

We have synthesized PtNTs and PtPdNTs (50 nm diameter, 5–20 μm long and 4–7 nm wall thickness) and tested their suitability as catalysts for ORR in PEMFCs. PtNTs were synthesized by a galvanic replacement reaction of silver nanowires (AgNWs) developed by Xia and co-workers.[5,6] The AgNWs were synthesized using a polyol method and subsequently heated at reflux with $Pt(CH_3COO)_2$ in an aqueous solution. After acid and heat treatment, the product was collected by centrifugation.

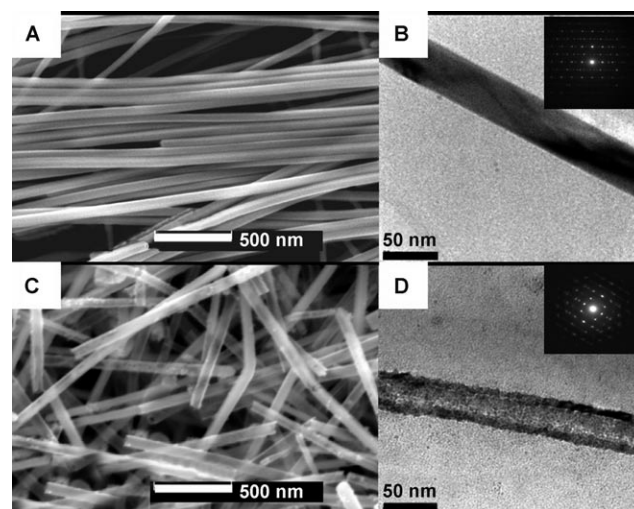The diameter (Figure 1 A,B) and length (Figure S4) of AgNWs are about 40 nm and 10 μm, respectively. The

Figure 1. A) SEM image of AgNWs. B) TEM image and electron diffraction pattern (inset) of AgNWs. C) SEM image of PtNTs. D) TEM image and electron diffraction pattern (inset) of PtNTs.

electron diffraction pattern (Figure 1 B, inset) shows that the AgNWs have a multiple-twinned structure. The diameter, wall thickness (Figure 1 C,D), and length (Figure S4) of the PtNTs are about 40 nm, 6 nm, and 10 μm, respectively. The electron diffraction pattern (Figure 1 D inset) of the PtNTs indicates that the walls of the tubes are polycrystalline. X-ray diffraction (XRD) patterns (Figure S5) show that PtNTs and PtPdNTs have been formed successfully. The face-centered cubic (fcc) lattice parameters of Pt/C, platinum black, PtNTs, and PtPdNTs are 0.3927, 0.3926, 0.3924, and 0.3897 nm, respectively.

The degradation of an electrocatalyst can be evaluated by repeated cyclic voltammetry (CV) cycles with the appropriate lower and upper potential limits in an acid solution.[2,4,7] Our durability tests were conducted by cycling the electrode

[*] Z. Chen, M. Waje, Dr. W. Li, Prof. Dr. Y. S. Yan
    Department of Chemical and Environmental Engineering
    Bourns College of Engineering
    Center for Environmental Research and Technology (CE-CERT)
    University of California, Riverside
    Riverside, CA 92521 (USA)
    Fax: (+1) 951-827-5696
    E-mail: yushan.yan@ucr.edu
    Homepage: http://www.engr.ucr.edu/faculty/chemenv/yusha-nyan.html

potential between 0 and 1.3 V versus a reversible hydrogen electrode (RHE) at a scan rate of 50 mV s^{-1} in an argon-purged $0.5 \text{M H}_2\text{SO}_4$ solution at 60 °C. The cyclic voltammograms for Pt/C (20 wt % platinum on Vulcan XC-72; E-TEK), platinum black (PtB; E-TEK), and PtNTs show a significant decrease of platinum ECSA for Pt/C and little reduction for PtNTs as the number of cycles increases (Figure 2A). The
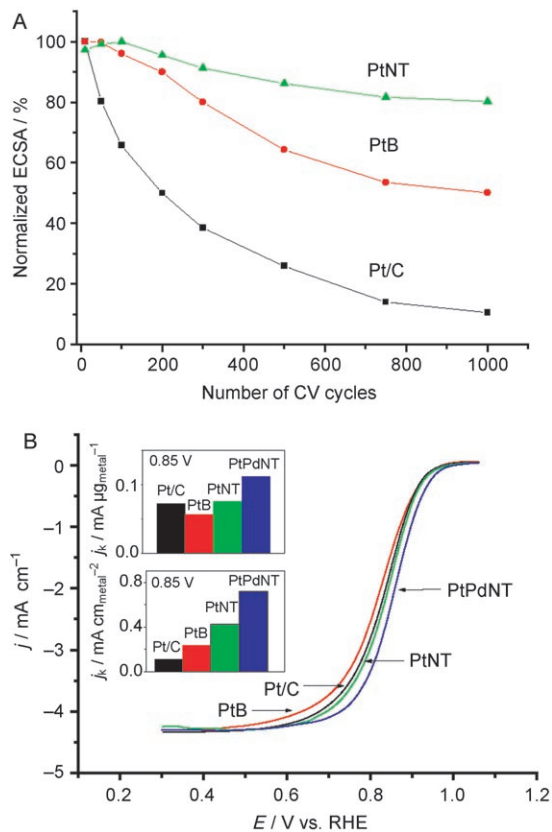

Figure 2. A) Loss of electrochemical surface area (ECSA) of Pt/C (E-TEK), platinum-black (PtB; E-TEK), and PtNT catalysts with number of CV cycles in Ar-purged $0.5 \text{M H}_2\text{SO}_4$ solution at 60 °C (0–1.3 V vs. RHE, sweep rate 50 mV s^{-1}). B) ORR curves (shown as current–voltage relations) of Pt/C, platinum black (PtB), PtNTs, and PdPtNTs in O_2-saturated $0.5 \text{M H}_2\text{SO}_4$ solution at room temperature (1600 rpm, sweep rate 5 mV s^{-1}). Inset: Mass activity (top) and specific activity (bottom) for the four catalysts at 0.85 V.

platinum ECSA of the PtNTs only decreases about 20 % even after 1000 cycles, while the platinum-black and Pt/C catalysts have lost about 51 and 90 % of their platinum ECSA, respectively.

The Pt/C, platinum-black, and PtNT catalysts were examined by TEM after the CV cycling (Figure S7). The platinum-nanoparticle size in the Pt/C catalyst increased from 2–5 to 10–20 nm (by about a factor of five) after the CV cycling (Figure S7 A,B), confirming that the major cause for the platinum ECSA loss of Pt/C is by platinum-nanoparticle ripening and possibly by aggregation owing to carbon corrosion. At the same time, the particle size of platinum black increased from 5–10 to 10–25 nm (Figure S7 C,D) after CV cycling, which demonstrates platinum-nanoparticle

growth driven by surface-energy minimization and Ostwald ripening. By contrast, there are no noticeable morphological changes for the PtNTs after the CV cycling (Figure S7 E,F). The small drop in platinum ECSA may be due to mild dissolution of platinum, because the other three mechanisms, namely, Ostwald ripening, aggregation, and carbon corrosion appear to be eliminated by the micrometer-sized length and the absence of the carbon support. A more detailed study to understand the quantitative contribution of each degradation mechanism using electrochemical methods is underway.

Figure 2B shows typical ORR polarization curves of Pt/C and PtNTs obtained at room temperature in O_2-saturated $0.5 \text{M H}_2\text{SO}_4$ using a rotating disk electrode (RDE) at 1600 rpm. The half-wave potentials of the PtNTs, platinum black, and Pt/C are 0.837, 0.817, and 0.828 V, respectively, showing that the activity of the PtNTs is higher than that of the commercial platinum-black and Pt/C catalysts. The insets in Figure 2B show that mass activity and specific activity are good indicators of an electrocatalyst's quality. PtNTs have a slightly higher mass activity but a significantly higher (3.8 times) specific activity than Pt/C at 0.85 V. Both the mass activity and the specific activity of the PtNTs are higher (1.4 and 1.8 times, respectively) than for the platinum black. The improved activity of the PtNTs might be due to the preferential exposure of certain crystal facets of the PtNTs.[4,8] The mass activity of the PtNTs can be further improved by reducing the wall thickness of the PtNTs and by employing platinum-alloy nanotubes.

To obtain higher mass activity and to take advantage of the higher activity offered by certain platinum alloys,[9] PtPdNTs were synthesized. The SEM and TEM images (Figure 3A,B) show the uniform diameter (45 nm), wall thickness (7 nm), and length (10 µm) of the PtPdNTs. The inset of Figure 3B shows an electron diffraction pattern of the PtPdNTs. The ORR curve (Figure 2B) shows that the half-wave potential of the PtPdNTs is 0.851 V, which is higher than that of the PtNTs, platinum black, and Pt/C. The mass activity of the PtPdNTs is 1.4 and 2.1 times higher than that of Pt/C and platinum black, respectively, and the specific activity of the PtPdNTs is even 5.8 and 2.7 times higher than that of the Pt/C and platinum-black electrocatalysts, respectively, at 0.85 V. The improved ORR kinetics of the PtPdNTs compared to PtNTs could be due to changes in the bond lengths, which are reflected in the different fcc lattice parameters shown by the XRD results and have also been suggested in the literature.[9]
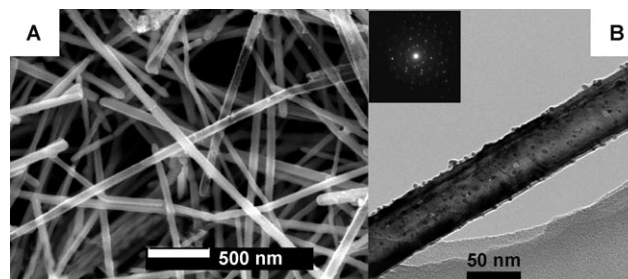

Figure 3. A) SEM image of PtPdNTs. B) TEM image and electron diffraction pattern (inset) of PtPdNTs.

Supportless platinum-black systems in the form of nano-particles (5–10 nm) were the first-generation PEMFC cata-lysts used in a practical system and are still used in space applications today. These catalysts are more durable than Pt/C but suffer from low surface area and low utilization, leading to expensive fuel cells. By taking advantage of the recent advances in nanotechnology, we demonstrate a new generation of supportless electrocatalysts based on PtNTs and PtPdNTs, which, because of their unique combination of dimensions, have the potential to combine the advantages of platinum-black and Pt/C catalysts while overcoming their drawbacks. Specifically they have the potential to possess high surface area, high utilization, high activity, and high durability. The optimization of the dimensions of the PtNTs and PtPdNTs and the preparation and performance testing of membrane–electrode assemblies (MEAs) based on PtNT and PtPdNT catalysts are underway.

Experimental Section

Silver nanowires were synthesized by reducing $AgNO_3$ with ethylene glycol (EG) in the presence of platinum seeds and poly(vinyl pyrrolidone) (PVP; $M_w \approx 40000$). In a typical synthesis, EG (50 mL) was heated in a three-necked round-bottom flask (equipped with a condenser, thermocontroller, and magnetic stirring bar) at 165°C for 1 h. Subsequently, H_2PtCl_6 solution (5 mL, 2×10^{-4} M in EG) was added. After 5 min, $AgNO_3$ solution (25 mL, 0.12 M in EG) and PVP solution (50 mL, 0.36 M in EG) were added dropwise (simultaneously) to the hot solution over 6 min, and the reaction continued at 165°C for 50 min. Vigorous stirring was maintained throughout the entire process. To purify the product, the reaction mixture was diluted with acetone (500 mL) and centrifuged at 3000 rpm for 15 min.[6,10]

In a typical PtNT synthesis, the reaction mixture containing the as-synthesized silver nanowires (5 mL) was diluted with water (100 mL) and subsequently heated at reflux for 10 min. Aqueous $Pt(CH_3COO)_2$ (50 mL, 1 mM) was slowly added dropwise to the refluxing solution over 15 min. The resulting mixture was maintained at the reflux temperature until its color became stable. Vigorous stirring was employed throughout all syntheses. Before PtNTs were used as catalysts, acid treatment and annealing treatment were needed. Acid treatment was performed in 0.5 M HNO_3 solution for 2 h with stirring. The PtNTs were separated by centrifugation and washing with doubly deionized H_2O and ethanol. The heat treatment was carried out under an Ar flow in an oven at 250°C for 1 h. For PtPdNTs preparation, aqueous $Pt(CH_3COO)_2$ (40 mL, 1 mM) and $Pd(NO_3)_2$ (10 mL, 1 mM) were used instead of aqueous $Pt(CH_3COO)_2$ (50 mL, 1 mM) as described above.

The electrochemical measurements were conducted in a thermo-stat-regulated standard electrochemical cell using a glassy carbon (GC) rotating disk electrode (RDE) setup with a multichannel potentiostat (VMP, Princeton Applied Research) and rotation control (MSR, Pine Instruments). Potentials were determined using a saturated Ag/AgCl electrode that was separated from the working electrode compartment by a closed electrolyte bridge. All potentials in this study, however, are given relative to the reversible hydrogen electrode (RHE). Figure S6 shows the preparation method of the working electrode.[8,11] In short, aqueous suspensions of 2 mg cata-lyst mL^{-1} were obtained by ultrasonic mixing for about 15 min. GC disk electrodes (5 mm diameter, 0.198 cm^2, AFE3T050GC, Pine Research Instrumentation) served as the substrate for the supported catalyst and were polished to a mirror finish (No. 40-7218 Microcloth, Buehler). An aliquot of catalyst suspension was transferred onto the carbon substrate, leading to a metal loading of 40 μg metal cm^{-2} for Pt/C, platinum black, PtNTs, and PdPtNTs. After evaporation of the water in air, 10 μL of a 0.05 wt% nafion solution (diluted from 5 wt% nafion, Ion Power Inc.) was transferred onto the electrode surface to attach the catalyst particles to the GC RDE, yielding a nafion film thickness of approximately 100 nm. Finally, the nafion-coated catalyst layer on the GC was heated at 120°C for 1 h in air.

The cyclic voltammetry (CV) test for accelerated durability was performed on the working electrode by cycling the voltage between 0 V and 1.3 V versus RHE in an Ar-purged 0.5 M aqueous H_2SO_4 solution at 60°C. The scan rate was 50 mVs^{-1}. The electrochemical surface areas were calculated from the H_2 desorption peak of the CV cycle. In total, 1000 CV cycles were performed for each case.

Transmission electron microscopy (TEM) was carried out on a PHILIPS CM300 instrument operating at 300 kV. Scanning electron microscopy (SEM) was conducted on a PHILIPS XL30-FEG instru-ment at 10 KV. X-ray diffraction (XRD) patterns were obtained on a Bruker D8 Advance Diffractometer (Bruker AXS) using $Cu_{K\alpha}$ radiation.

[1] a) P. J. Ferreira, G. J. la O', Y. Shao-Horn, D. Morgan, R. Makharia, S. Kocha, H. A. Gasteiger, *J. Electrochem. Soc.* **2005**, *152*, A2256; b) J. Xie, D. L. Wood, D. M. Wayne, T. A. Zawodzinski, P. Atanassov, R. L. Borup, *J. Electrochem. Soc.* **2005**, *152*, A104.

[2] J. Zhang, K. Sasaki, E. Sutter, R. R. Adzic, *Science* **2007**, *315*, 220.

[3] a) K. Lee, J. J. Zhang, H. J. Wang, D. P. Wilkinson, *J. Appl. Electrochem.* **2006**, *36*, 507; b) C. Wang, M. Waje, X. Wang, J. M. Tang, R. C. Haddon, Y. S. Yan, *Nano Lett.* **2004**, *4*, 345; c) X. Wang, W. Z. Li, Z. W. Chen, M. Waje, Y. S. Yan, *J. Power Sources* **2006**, *158*, 154.

[4] M. K. Debe, A. K. Schmoeckel, G. D. Vernstrorn, R. Atana-soski, *J. Power Sources* **2006**, *161*, 1002.

[5] B. Mayers, X. C. Jiang, D. Sunderland, B. Cattle, Y. N. Xia, *J. Am. Chem. Soc.* **2003**, *125*, 13364.

[6] a) Y. G. Sun, Z. L. Tao, J. Chen, T. Herricks, Y. N. Xia, *J. Am. Chem. Soc.* **2004**, *126*, 5940; b) Y. G. Sun, B. Wiley, Z. Y. Li, Y. N. Xia, *J. Am. Chem. Soc.* **2004**, *126*, 9399; c) Y. G. Sun, Y. D. Yin, B. T. Mayers, T. Herricks, Y. N. Xia, *Chem. Mater.* **2002**, *14*, 4736; d) Y. N. Xia, P. D. Yang, Y. G. Sun, Y. Y. Wu, B. Mayers, B. Gates, Y. D. Yin, F. Kim, Y. Q. Yan, *Adv. Mater.* **2003**, *15*, 353.

[7] a) A. Kongkanand, S. Kuwabata, G. Girishkumar, P. Kamat, *Langmuir* **2006**, *22*, 2392; b) M. K. Debe, A. K. Schmoeckel, R. Atanasoski, G. D. Vernstrom, Abstract 64, Fuel Cell Seminar, Palm Springs, November 14–18, **2005**.

[8] U. A. Paulus, T. J. Schmidt, H. A. Gasteiger, R. J. Behm, *J. Electroanal. Chem.* **2001**, *495*, 134.

[9] a) J. L. Fernandez, V. Raghuveer, A. Manthiram, A. J. Bard, *J. Am. Chem. Soc.* **2005**, *127*, 13100; b) J. Zhang, F. H. B. Lima, M. H. Shao, K. Sasaki, J. X. Wang, J. Hanson, R. R. Adzic, *J. Phys. Chem. B* **2005**, *109*, 22701; c) J. Zhang, Y. Mo, M. B. Vukmirovic, R. Klie, K. Sasaki, R. R. Adzic, *J. Phys. Chem. B* **2004**, *108*, 10955; d) J. L. Zhang, M. B. Vukmirovic, K. Sasaki, A. U. Nilekar, M. Mavrikakis, R. R. Adzic, *J. Am. Chem. Soc.* **2005**, *127*, 12480; e) J. L. Zhang, M. B. Vukmirovic, Y. Xu, M. Mavrikakis, R. R. Adzic, *Angew. Chem.* **2005**, *117*, 2170; *Angew. Chem. Int. Ed.* **2005**, *44*, 2132.

[10] a) Y. G. Sun, B. Mayers, Y. N. Xia, *Adv. Mater.* **2003**, *15*, 641; b) Y. G. Sun, B. T. Mayers, Y. N. Xia, *Nano Lett.* **2002**, *2*, 481.

[11] E. Higuchi, H. Uchida, M. Watanabe, *J. Electroanal. Chem.* **2005**, *583*, 69.